

# 1D POLYMERIC IODOANTIMONATES(III) WITH 1-METHYLPYRIDINIUM AND 3-BROMO-1-METHYLPYRIDINIUM CATIONS: STRUCTURES AND PROPERTIES

© 2025 I. A. Shentseva<sup>a</sup>, A. N. Usol'tsev<sup>a</sup>, N. A. Korobeinikov<sup>a, b, \*</sup>, and S. A. Adonin<sup>a, c</sup>

<sup>a</sup>Nikolaev Institute of Inorganic Chemistry, Siberian Branch, Russian Academy of Sciences, Novosibirsk, Russia

<sup>b</sup>Novosibirsk State University, Novosibirsk, Russia

<sup>c</sup>Favorskii Institute of Chemistry, Siberian Branch, Russian Academy of Sciences, Irkutsk, Russia

\*e-mail: korobeynikov@niic.nsc.ru

Received May 15, 2024

Revised June 05, 2024

Accepted June 05, 2024

**Abstract.** The reactions of SbI<sub>3</sub> with iodides of cations of the pyridinium family in a mixture of acetonitrile and acetone afford two polymeric iodoantimonate complexes: (1-MePy)[SbI<sub>4</sub>] (I) and (3-Br-1-MePy)[SbI<sub>4</sub>] (II). Specific features of the crystal structures are determined by X-ray diffraction (XRD). The thermal stability of compounds I and II is evaluated by thermogravimetry. The optical forbidden bandgaps are estimated from the diffuse reflectance spectra.

**Keywords:** XRD, complexes, halide complexes, noncovalent interactions, antimony

**DOI:** 10.31857/S0132344X250102e5

## INTRODUCTION

The study of halide complexes of bismuth(III) [1–6], stibium(III) [7–9] and other p-elements [10–14] is one of the interesting directions for both coordination chemistry and materials science. It is related to attempts to create photocatalytic systems [15–19], light-emitting devices [20–22] and photodetectors [23, 24]. Of particular interest are works in the field of so-called perovskite solar cells, which have been developed in the last decade [25, 26]. Most of the work in this direction is based on the use of lead(II) compounds, but its toxicity and relatively low photostability of the resulting complexes (especially in the form of films) are factors limiting further development of this area. This stimulates the study of the possibility of using halogenometallates of other p-elements in photovoltaic devices [27–31].

In addition to applied aspects, halide compounds are of considerable interest from the point of view of fundamental chemistry because of the extraordinary variety of structures of complex anions of both discrete and polymeric structure [8, 32, 33]. The most important factor influencing the composition, structure and, as a consequence, the properties of metal halide complexes is the nature of the cation. Nevertheless, the general structure–property regularities, which allow to create GMs with given properties, are still unknown. The only

method of study remains the study of compounds with structurally related cations. In this respect, pyridine derivatives and other nitrogen-containing heterocyclic compounds, commercially available and easily modifiable, are suitable for synthesis. The presence of halogen-substituted cations capable of noncovalent interaction with metal anion complexes – halogen bond (HB) [34–38] is worth noting separately. The influence of this factor is being actively studied, including its application in photovoltaic systems [39, 40].

According to the Cambridge Structural Database, the number of structurally characterized studied stibium iodide complexes is much smaller than that of iodobismutates (III). As part of the study of the regularities of the formation of new halide complexes of p-elements, we obtained two stibium(III) complexes, (1-MePy)[SbI<sub>4</sub>] (I) and (3-Br-1-MePy)[SbI<sub>4</sub>] (II). The features of the crystal structure and non-covalent contacts in it were studied by X-ray diffraction analysis (XRD). The thermal stability was studied by thermogravimetric analysis (TGA). From the diffuse reflectance spectra, the forbidden band was evaluated.

## EXPERIMENTAL PART

The preparation of compounds I and II was carried out in air. Iodide salts of 1-methylpyridinium and 3-bromo-1-methylpyridinium were prepared

by interaction of the corresponding organic bases (pyridine – VECTON JSC, 99%; 3-bromopyridine – SigmaAldrich, 99%) with methyl iodide (Chemical Line, “pure”) in acetonitrile (VECTON JSC, “pure for analysis”) under heating at 70°C for 24 hours. Stibium(III) iodide was prepared by interaction of metallic stibium and crystalline iodine in boiling toluene.

**Synthesis of (1-MePy){[SbI<sub>4</sub>]}** (I). 50 mg of SbI<sub>3</sub> (0.10 mmol) and 24 mg (0.10 mmol) of 1-methylpyridinium iodide were dissolved in 7 mL of an acetonitrile-acetone (1:1) solvent mixture at 70°C for 1 h over heat. After dissolution, the mixture was slowly cooled to room temperature and incubated for 24 hours. After partial evaporation of the solvent, orange crystals were obtained. The yield was 55%.

**Synthesis of (3-Br-1-MePy){[SbI<sub>4</sub>]}** II. 50 mg of SbI<sub>3</sub> (0.10 mmol) and 30 mg (0.10 mmol) of 3-bromo-1-methylpyridinium iodide were dissolved in 15 mL of an acetonitrile-acetone (1:1) solvent mixture at 70°C under heat for 1 h. After dissolution, the mixture was slowly cooled to room temperature and incubated for 24 hours. After partial evaporation of the solvent, orange crystals were obtained. The yield was 50%.

Found, %: C 9.72; N<sub>1.30</sub>; N1.89.

For C<sub>6</sub>H<sub>8</sub>NI<sub>4</sub>Sb (I)

calculated, %: C 9.96; N1.11; N1.94.

Found, %: C 8.79; N<sub>1.10</sub>; N1.79.

For C<sub>6</sub>H<sub>7</sub>NBrI<sub>4</sub>Sb (II)

calculated, %: C 8.98; N0.88; N1.75.

**XRD** of the single crystals I and II was carried out at 150 K on a Bruker D8 Venture diffractometer with a CMOS PHOTON III detector (graphite monochromator,  $MoK_{\alpha}$ -radiation,  $\lambda = 0.71073$  Å,  $\phi$ - and  $\omega$ -scanning). Integration, absorption recording, and determination of unit cell parameters were carried out using the CrysAlisPro software package. The structures of compounds I and II were deciphered using the SHELXT software [41] and refined by the full-matrix least-squares method in the anisotropic approximation for non-hydrogen atoms using the SHELXL 2017\1 algorithm [42] in the Olex2 software [43]. The positions of the hydrogen atoms of the organic fragments were calculated geometrically and refined using the “rider” model. The crystallographic data and details of the experiments are summarized in Table 1.

The crystallographic parameters of the complexes I and II have been deposited in the Cambridge Structural Database (CCDC No. 2346399 and 2346400, respectively; <https://www.ccdc.cam.ac.uk/structures/>).

**X-ray phase analysis (XRF).** Data of powder X-ray phase analysis were obtained on Bruker D8 Advance diffractometer ( $CuK_{\alpha}$ -radiation, LYNXEYE XE-T linear detector, 2θ range of 4°–50°, 0.03° 2θ step, accumulation time 0.5 s/step). Samples for the study

were prepared as follows: a polycrystalline sample was ground in an agate mortar in the presence of heptane, the resulting suspension was applied to the polished side of a standard quartz cuvette. After drying of the heptane, the sample was a thin even layer. All peaks in the diffractograms of the compounds I and II were indexed by X-ray diffraction analysis, the samples are single phase.

TGA was performed on a TG 209 F1 (Iris instrument, Germany). The measurements were carried out in helium flow in the temperature range of 25–450°C at a gas flow of 60 ml/min, heating rate of 10 deg/min in open aluminum crucibles.

**Optical properties.** Spectra for powders I and II were measured using a system consisting of a Kolibri-2 spectrometer (VMK Optoelektronika, Russia), a QR-400-7 reflection/reverse scattering probe (Ocean Optics, USA), and an AvaLight-DHS deuterium-tungsten lamp (Avantes, Netherlands).

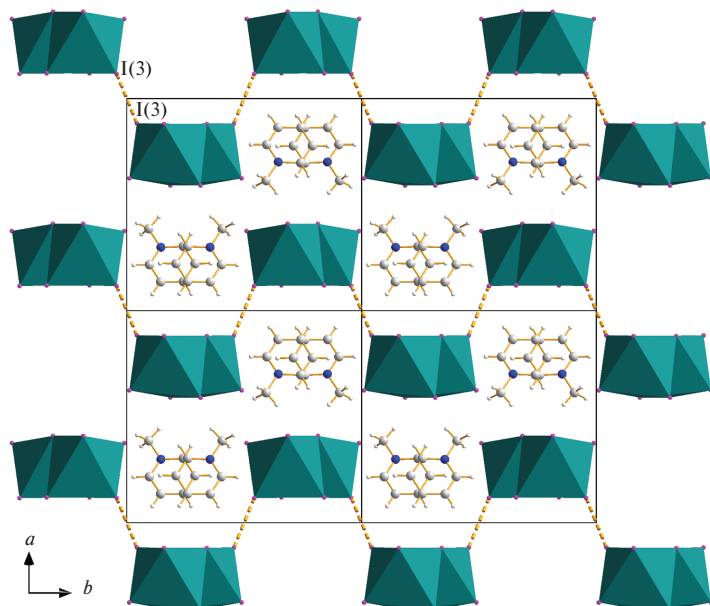
## RESULTS AND DISCUSSION

The compounds I and II were prepared using a common approach for halogenometallates. The independent part of the structure contains one cation and one monomeric fragment {SbI<sub>4</sub>}. These fragments are linked via common  $\mu_2$ -type bridging iodide ligands into one-dimensional zigzag polymer chains. In the chemistry of stibium(III) iodide complexes, this structural type is represented in the literature by several examples [27, 28, 44]. In the structure of the compound I, the polymer chains are arranged along the crystallographic *c*-axis. The distances Sb–I<sub>term</sub> are 2.8064(4), 2.8371(4) Å, Sb–I $\mu$ 2 are 3.1172(4)–3.3915(4) Å. The main feature of I is the presence of short I · · · I contacts at a distance of 3.7461(4) Å (Fig. 1), which is noticeably smaller than the sum of van der Waals radii for iodine atoms (3.96 Å [45]). A number of stibium compounds with shorter contacts between the iodine atoms [46–49] with the smallest one in the compound (HPyz)<sub>3</sub>Sb<sub>2</sub>I<sub>9</sub> · 2H<sub>2</sub>O (3.646 Å at 100 K, 3.530 Å at 230 K) [50] were identified by analyzing the Cambridge Structural Database.

The presence of halogen atoms in the cation of the compound II leads to a markedly greater variety of noncovalent contacts. In addition to interactions between iodine atoms (I(4) · · · I(4), 3.8167(4) Å), Br · · · I contacts link one of the terminal iodine atoms and the cation at a distance of 3.7271(6) Å (see Fig. 2; the sum of van der Waals radii of Br and I is 3.81 Å [45]). Analysis of the geometry of noncovalent interactions in the compounds allows us to attribute the contacts between iodine atoms to HB of the first type [51], related to crystal packing effects. For example, in the compound I, the corresponding angle is 136.860(8)° (Sb(1)–I(3) · · · I(3)). The Br · · · I contact in the compound II can be considered as a type II HB – the corresponding angles are 160.375(104)° (C(3)–Br(1) · · · I(5) and 117.71(1)° (Sb(1)–I(5) · · · Br(1)). The

**Table 1.** Crystallographic data, experimental parameters and refinements of the structures I and II

Parameter	I	II
Gross formula	$I_4Sb \cdot C_6H_8N$	$I_4Sb \cdot C_6H_7BrN$
M	723.48	802.39
Syngony, sp. group	Monoclinic, $P2_1/c$	Triclinic, $P\bar{I}^-$
$a, \text{\AA}$	13.2179 (9)	7.8193 (5)
$b, \text{\AA}$	14.0855 (10)	9.4759 (6)
$c, \text{\AA}$	7.8400 (5)	10.9448 (6)
$\alpha, \beta, \gamma, \text{deg}$	90, 105.768 (2), 90	74.005 (2), 85.411 (2), 83.868 (2)
$V, \text{\AA}^3$	1404.73 (17)	774.01 (8)
Z	4	2
$\rho_{(\text{calc.})}, \text{g cm}^{-3}$	3.421	3.443
$\mu, \text{mm}^{-1}$	10.72	12.31
$F(000)$	1256	696
Crystal size, mm	0.19 $\times$ 0.1 $\times$ 0.09	0.12 $\times$ 0.08 $\times$ 0.05
Index range $hkl$	$-18 \leq h \leq 17, -18 \leq k \leq 19, -10 \leq l \leq 10$	$-11 \leq h \leq 11, -13 \leq k \leq 13, -15 \leq l \leq 15$
Data acquisition area in $\theta$ , deg	2.892–29.596	1.938–30.539
$(\sin \theta / \lambda)_{\text{max}}, \text{\AA}^{-1}$	0.695	0.715
Measured reflections	17093	15132
Independent reflections	3846	4719
Reflections with $I > 2\sigma(I)$	3736	4277
$R_{\text{int}}$	0.032	0.035
Number of parameters to be specified/number of constraints	110/0	119/0
R-factor (all data)	$R_1 = 0.0221, wR_2 = 0.0470$	$R_1 = 0.0271, wR_2 = 0.0487$
R-factor ( $I > 2\sigma(I)$ )	$R_1 = 0.0211, wR_2 = 0.0467$	$R_1 = 0.0238, wR_2 = 0.0473$
GOOF by $F^2$	1.287	1.058
Residual electron density (max/min), $e/\text{\AA}^3$	0.77/-0.71	1.41/-1.92

**Fig. 1.** Crystal packing of the compound I along the crystallographic axis  $c$ .

Sb-I<sub>term</sub> distances in II are 2.8300(3)-2.8333(3) Å, Sb-I<sub>μ2</sub> distances are 2.9886(3)-3.3065(3) Å.

Stacking interactions between cations in the obtained structures form parallel chains along the *c* and *a* axes, respectively (Fig. 3). The C · · · C distances in

the compound I are 3.5284(61)-3.5894(61) Å, C · · · N distances are 3.5304(54)-3.7820(54) Å. In II we cannot find equally short C · · · C and C · · · N contacts, but there are contacts involving the Br atom (C · · · Br 3.4384(32)-3.8883(37) Å, N · · · Br 3.5703(24) Å).

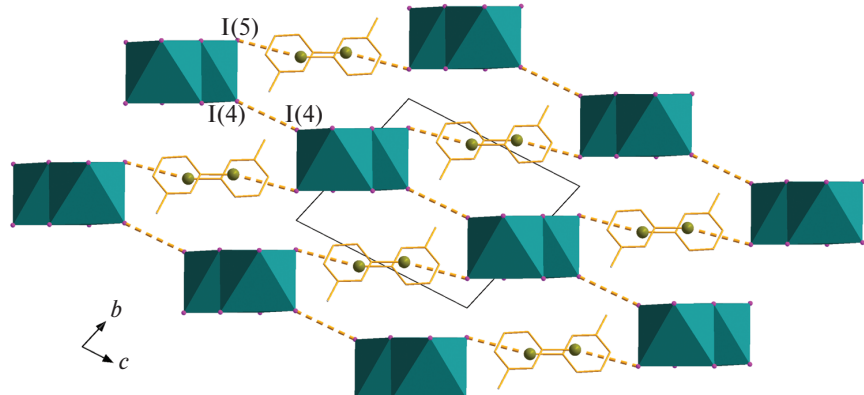


**Fig. 2.** Br···I and I···I contacts (dashed line) in the crystal structure II. Hydrogen atoms are not shown.

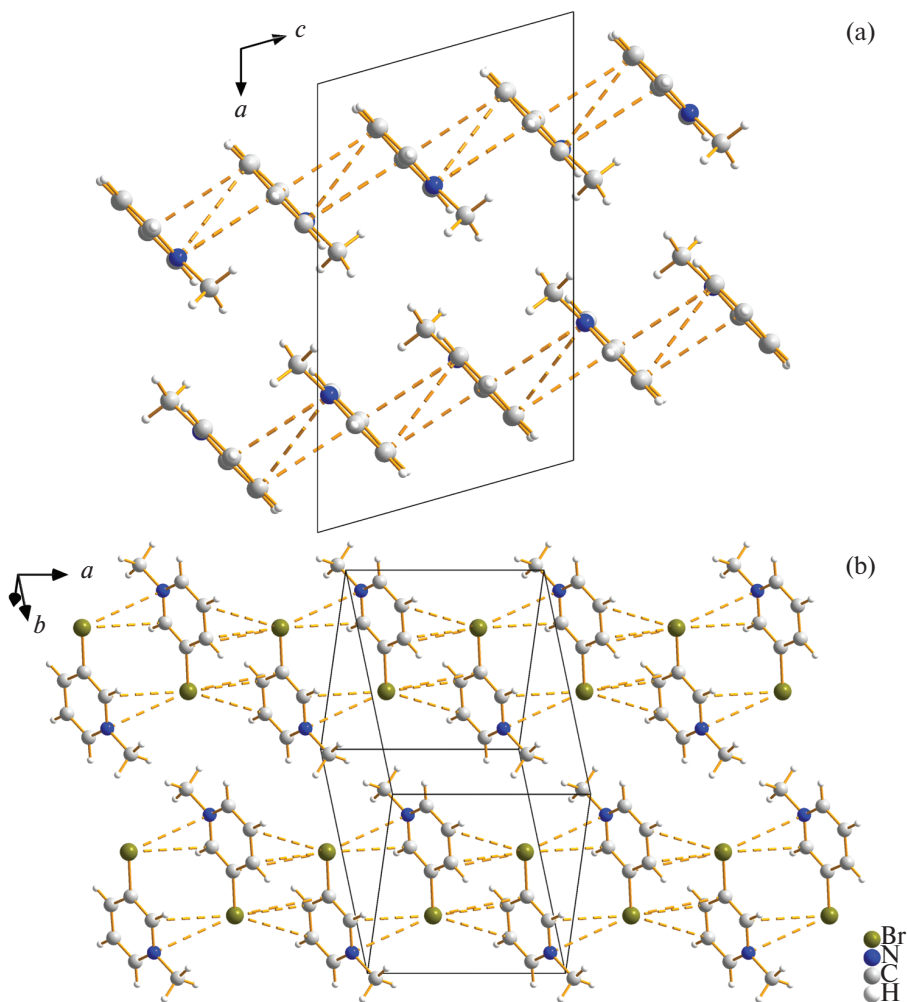


**Fig. 3.** Stacking interactions in the structures of the compounds I (a) and II (b).

Fig. 4 compares the experimental diffractograms with the calculated ones. The compounds were obtained in pure form. The thermal stability, an important parameter for any applications, was evaluated by the TGA method. The decomposition of the complexes I and II starts at  $\sim 200^\circ\text{C}$ , occurs in

one stage without noticeable steps and is completely terminated at temperatures around  $350$  and  $300^\circ\text{C}$  (Fig. 5).

The diffuse reflectance spectrum and determination of the forbidden zone width (FZW)

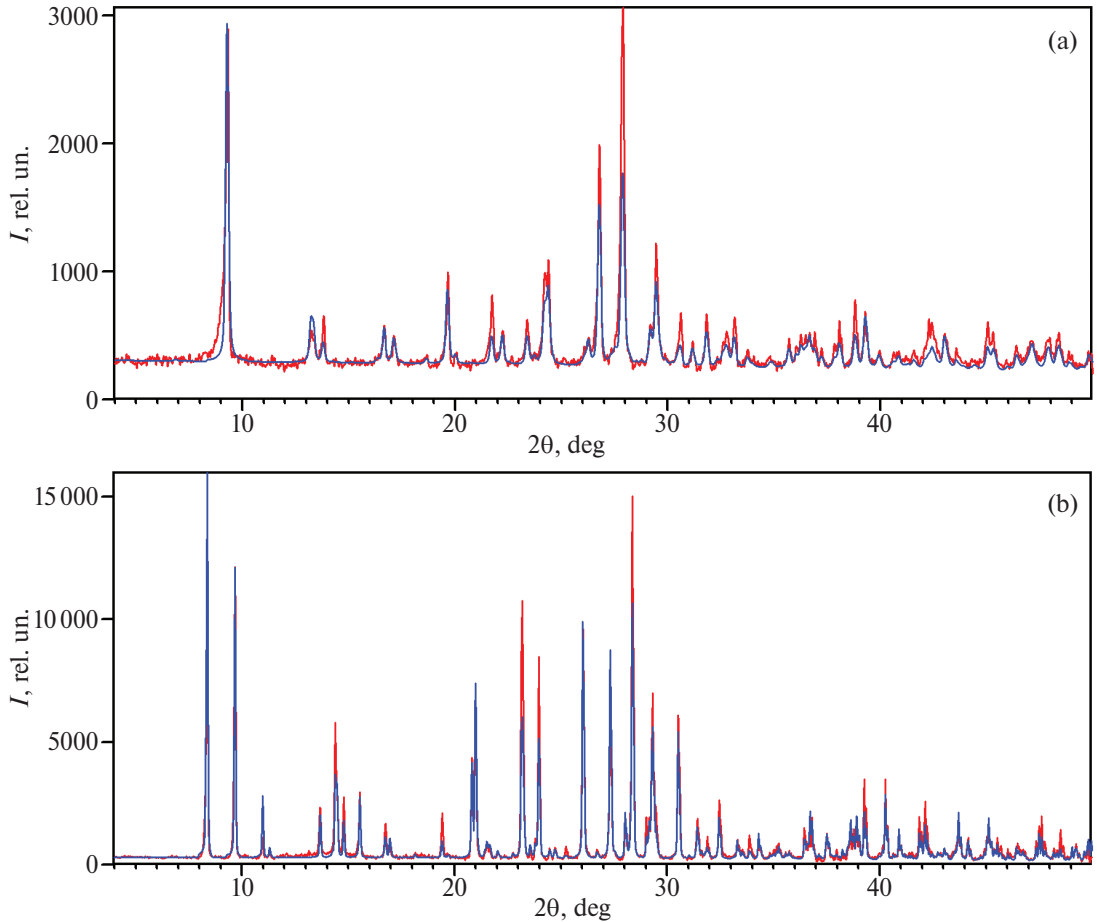


Fig. 4. Powder diffractograms of the compounds I (a) and II (b): calculated (blue) and experimental (red).

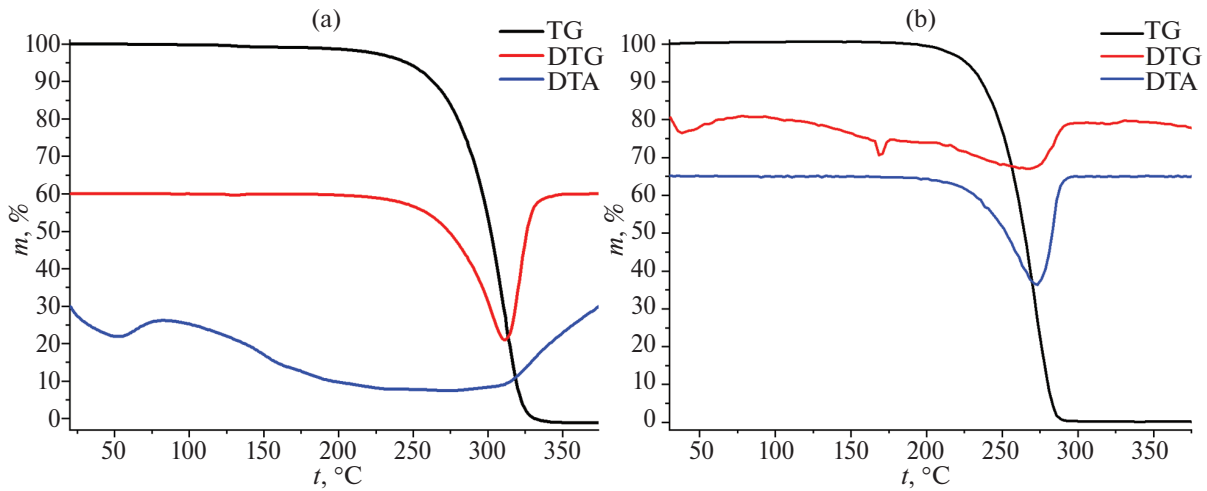
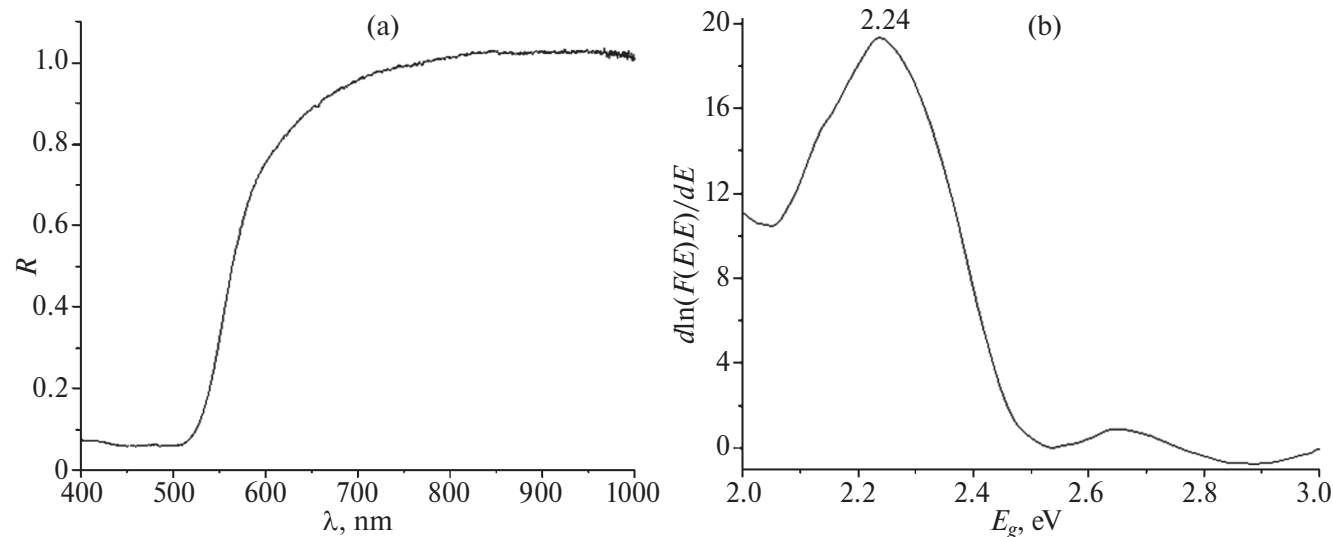


Fig. 5. TG, DTG and DTA curves for compounds I (a) and II (b).



**Fig. 6.** Diffuse reflectance spectra (left) of compounds and calculation of the forbidden band width (right) for the compound I.

(Fig. 6) according to the method of Bhattacharyya et al. [52] gives values of 2.24 and 2.15 eV for I and II, respectively, which is in agreement with literature data; the values of FZW for Sb(III) iodide complexes can vary in wide ranges: from a record low 1.55 eV [44] to almost 2.5 eV [53].

Two new stibium(III) compounds with cations – pyridine derivatives have been synthesized and structurally characterized as a result of these studies. In the crystal structure of compound II, the presence of noncovalent interactions between the halogen atoms of the cation and the anionic part can be noted. Both complexes exhibit rather high thermal stability.

#### CONFLICT OF INTEREST

The authors declare that they have no conflict of interest.

#### ACKNOWLEDGEMENTS

The authors thank T.S. Sukhikh for providing the data measured in the X-ray diffraction Shared-use Center at the Nikolaev Institute of Inorganic Chemistry, RAS. The authors thank I.V. Korolkov for conducting the powder diffraction experiments. The authors thank the Ministry of Science and Higher Education of the Russian Federation (structural characterization of samples, State Assignment No. 121031700313-8).

#### FUNDING

This work was supported by the Russian Science Foundation (project No. 23-73-10054)

#### REFERENCES

1. Sharutin V.V., Egorova I.V., Klepikov N.N. et al. // Russ. J. Inorg. Chem. 2009. V. 54. No. 11. P. 1768. <https://doi.org/10.1134/S0036023609110126>
2. Buikin P.A., Rudenko A.Y., Ilyukhin A.B. et al. // Russ. J. Coord. Chem. 2020. V. 46. No. 2. P. 111. <https://doi.org/10.1134/S1070328420020049>
3. Buikin P.A., Rudenko A.Y., Baranchikov A.E. et al. // Russ. J. Coord. Chem. 2018. V. 44. No. 6. P. 373. <https://doi.org/10.1134/S1070328418060015>
4. Chen Y., Yang Z., Guo C.X. et al. // Eur. J. Inorg. Chem. 2010. No. 33. P. 5326. <https://doi.org/10.1002/ejic.201000755>
5. Möbs J., Gerhard M., Heine J. // Dalton Trans. 2020. V. 49. No. 41. P. 14397. <https://doi.org/10.1039/d0dt03427d>
6. Hrizi C., Trigui A., Abid Y. et al. // J. Solid State Chem. 2011. V. 184. No. 12. P. 3336. <https://doi.org/10.1016/j.jssc.2011.10.004>
7. Sharutin V.V., Pakusina A.P., Sharutina O.K. et al. // Russ. J. Coord. Chem. 2004. V. 30. No. 8. P. 541. <https://doi.org/10.1023/B:RUCO.0000037432.61330.07>
8. Möbs J., Stuhrmann G., Weigend F. et al. // Chem. Eur. J. 2022. <https://doi.org/10.1002/chem.202202931>
9. Zhao J.-Q., Shi H.-S., Zeng L.-R. et al. // Chem. Eng. J. 2022. V. 431. <https://doi.org/10.1016/j.cej.2021.134336>
10. Feng L.-J., Zhao Y.-Y., Song R.-Y. et al. // Inorg. Chem. Commun. 2022. V. 136. <https://doi.org/10.1016/j.inoche.2021.109146>
11. Fateev S.A., Petrov A.A., Khrustalev V.N., et al. // Chem. Mater. 2018. V. 30. No. 15. P. 5237. <https://doi.org/10.1021/acs.chemmater.8b01906>

12. *Petrov A.A., Marchenko E.I., Fateev S.A. et al.* // Mendeleev Commun. 2022. V. 32. No. 3. P. 311. <https://doi.org/10.1016/j.mencom.2022.05.006>
13. *Fateev S.A., Stepanov N.M., Petrov A.A. et al.* // Russ. J. Inorg. Chem. 2022. V. 67. No. 7. P. 992. <https://doi.org/10.1134/S0036023622070075>
14. *Fateev S.A., Khrustalev V.N., Simonova A.V. et al.* // Russ. J. Inorg. Chem. 2022. V. 67. No. 7. P. 997. <https://doi.org/10.1134/S0036023622070087>
15. *Zhang Q., Wu Y., Fu H. et al.* // J. Colloid Interface Sci. 2024. V. 664. No. March. P. 809. <https://doi.org/10.1016/j.jcis.2024.03.057>
16. *Huang Y., Yu J., Wu Z. et al.* // RSC Adv. 2024. V. 14. No. 7. P. 4946. <https://doi.org/10.1039/d3ra07998h>
17. *Chen Z., Hu Y., Wang J. et al.* // Chem. Mater. 2020. V. 32. No. 4. P. 1517. <https://doi.org/10.1021/acs.chemmater.9b04582>
18. *Dai Y., Poidevin C., Ochoa-Hernández C. et al.* // Angew. Chem. Int. Ed. 2020. V. 59. No. 14. P. 5788. <https://doi.org/10.1002/anie.201915034>
19. *Wu L.Y., Mu Y.F., Guo X.X. et al.* // Angew. Chem. Int. Ed. 2019. V. 58. No. 28. P. 9491. <https://doi.org/10.1002/anie.201904537>
20. *Lin K., Xing J., Quan L.N. et al.* // Nature. 2018. V. 562. No. 7726. P. 245. <https://doi.org/10.1038/s41586-018-0575-3>
21. *Igbari F., Wang Z.K., Liao L.S.* // Adv. Energy Mater. 2019. V. 9. No. 12. P. 1. <https://doi.org/10.1002/aenm.201803150>
22. *Stranks S.D., Snaith H.J.* // Nat. Nanotechnol. 2015. V. 10. No. 5. P. 391. <https://doi.org/10.1038/nnano.2015.90>
23. *Li X., Shi J., Chen J. et al.* // Materials (Basel). 2023. V. 16. No. 12. <https://doi.org/10.3390/ma16124490>
24. *Lei Y., Wang S., Xing J. et al.* // Inorg. Chem. 2020. V. 59. No. 7. P. 4349. <https://doi.org/10.1021/acs.inorgchem.9b03277>
25. *Kojima A., Teshima K., Shirai Y. et al.* // J. Am. Chem. Soc. 2009. V. 131. No. 17. P. 6050. <https://doi.org/10.1021/ja809598r>
26. *Green M.A., Dunlop E.D., Hohl-Ebinger J. et al.* // Prog. Photovoltaics Res. Appl. 2022. V. 30. No. 7. P. 687. <https://doi.org/10.1002/pip.3595>
27. *Hu Y.Q., Hui H.Y., Lin W.Q. et al.* // Inorg. Chem. 2019. V. 58. No. 24. P. 16346. <https://doi.org/10.1021/acs.inorgchem.9b01439>
28. *Dennington A.J., Weller M.T.* // Dalton Trans. 2018. V. 47. No. 10. P. 3469. <https://doi.org/10.1039/c7dt04280a>
29. *Mastryukov M.V., Son A.G., Tekshina E.V. et al.* // Russ. J. Inorg. Chem. 2022. V. 67. No. 10. P. 1652. <https://doi.org/10.1134/S0036023622100540>
30. *Liu H., Zhang Z., Zuo W. et al.* // Adv. Energy Mater. 2023. V. 13. No. 3. <https://doi.org/10.1002/aenm.202202209>
31. *Pai N., Chatti M., Fürer S.O. et al.* // Adv. Energy Mater. 2022. V. 12. No. 32. P. 2201482. <https://doi.org/10.1002/aenm.202201482>
32. *Adonin S.A., Sokolov M.N., Fedin V.P.* // Coord. Chem. Rev. 2016. V. 312. P. 1. <https://doi.org/10.1016/J.CCR.2015.10.010>
33. *Wu L.-M., Wu X.-T., Chen L.* // Coord. Chem. Rev. 2009. V. 253. No. 23–24. P. 2787. <https://doi.org/10.1016/J.CCR.2009.08.003>
34. *Desiraju G.R., Shing Ho P., Kloo L. et al.* // Pure Appl. Chem. 2013. V. 85. No. 8. P. 1711. <https://doi.org/10.1351/PAC-REC-12-05-10>
35. *Suslonov V.V., Soldatova N.S., Ivanov D.M. et al.* // Cryst. Growth Des. 2021. V. 21. No. 9. P. 5360. <https://doi.org/10.1021/acs.cgd.1c00654>
36. *Eliseeva A.A., Ivanov D.M., Rozhkov A.V. et al.* // JACS Au. 2021. V. 1. No. 3. P. 354. <https://doi.org/10.1021/jacsau.1c00012>
37. *Bokach N.A., Suslonov V.V., Eliseeva A.A. et al.* // CrystEngComm. 2020. V. 22. No. 24. P. 4180. <https://doi.org/10.1039/c6ra90077a>
38. *Soldatova N.S., Postnikov P.S., Suslonov V.V. et al.* // Org. Chem. Front. 2020. V. 7. No. 16. P. 2230. <https://doi.org/10.1039/d0qo00678e>
39. *Kubasov A.S., Avdeeva V.V.* // 2024. No. Ii. P. 12.
40. *Ball M.L., Milić J.V., Loo Y.L.* // Chem. Mater. 2022. V. 34. No. 6. P. 2495. <https://doi.org/10.1021/acs.chemmater.1c03117>
41. *Sheldrick G.M.* // Acta Crystallogr. A. 2015. V. 71. No. 1. P. 3. <https://doi.org/10.1107/S2053273314026370>
42. *Sheldrick G.M.* // Acta Crystallogr. C. 2015. V. 71. No. 1. P. 3. <https://doi.org/10.1107/S2053229614024218>
43. *Dolomanov O.V.O. V., Bourhis L.J.L.J., Gildea R.J.R.J. et al.* // J. Appl. Crystallogr. 2009. V. 42. No. 2. P. 339. <https://doi.org/10.1107/S0021889808042726>
44. *Oswald I.W.H., Mozur E.M., Moseley I.P. et al.* // Inorg. Chem. 2019. V. 58. No. 9. P. 5818. <https://doi.org/10.1021/acs.inorgchem.9b00170>
45. *Mantina M., Chamberlin A.C., Valero R. et al.* // J. Phys. Phys. Chem. A. 2009. V. 113. No. 19. P. 5806. <https://doi.org/10.1021/JP8111556>
46. *Pohl S., Lotz R., Saak W. et al.* // Angew. Chem. Int. Ed. English. 1989. V. 28. No. 3. P. 344. <https://doi.org/10.1002/anie.198903441>
47. *Janczak J., Perpétuo G.J.* // Acta Crystallogr. C. 2006. V. 62. No. 7. P. M323. <https://doi.org/10.1107/S010827010601910X>
48. *Li Y., Xu Z., Liu X. et al.* // Inorg. Chem. 2019. V. 58. No. 9. P. 6544. <https://doi.org/10.1021/acs.inorgchem.9b00718>
49. *Sharutin V.V., Senchurin V.S., Sharutina O.K. et al.* // Russ. J. Inorg. Chem. 2011. V. 56. No. 10. P. 1561. <https://doi.org/10.1134/S0036023611100196>
50. *Möbs J., Stuhrmann G., Wippermann S. et al.* // ChemPlusChem. 2023. V. 88. No. 6. P. E202200403.
51. *Cavallo G., Metrangolo P., Milani R. et al.* // Chem. Rev. 2016. V. 116. No. 4. P. 2478. <https://doi.org/10.1021/acs.chemrev.5b00484>

52. *Bhattacharyya D., Chaudhuri S., Pal A.* // Vacuum. 1992. V. 43. No. 4. P. 313. [https://doi.org/10.1016/0042-207X\(92\)90163-Q](https://doi.org/10.1016/0042-207X(92)90163-Q)

53. *Mousdis G.A., Ganopoulos N.M., Barkaoui H. et al.* // Eur. J. Inorg. Chem V P. 2017.. 2017. No. 28. 3401. <https://doi.org/10.1002/.201700277>